J Mol Model (2013) 19:871–878
DOI 10.1007/s00894-012-1618-6

ORIGINAL PAPER

Partial activation of α7 nicotinic acetylcholine receptors: insights from molecular dynamics simulations

Caijuan Shi · Rilei Yu · Shengjuan Shao · Yanni Li

Received: 29 March 2012 / Accepted: 30 September 2012 / Published online: 20 October 2012

Abstract Nicotinic acetylcholine receptors (nAChRs) are drug targets for neuronal disorders and diseases. Partial agonists for nAChRs are currently being developed as drugs for the treatment of neurological diseases for their relative safety originated from reduced excessive stimulation. In the current study, molecular docking, molecular dynamics simulations and binding energy calculations were performed to theoretically investigate the interactions between the partial agonists, 4-OH-DMXBA and tropisetron with α7-nAChR. The results suggest that the partial agonists 4-OH-DMXBA and tropisetron bind with α7-nAChR in a binding mode similar to that with AChBP. The non-conserved residues in the binding sites contribute to the orientation deviation of these partial agonists from their orientation in AChBP. Energy calculation and decomposition using MM-GB/SA suggests that the van der Waals term (ΔE_{VDW}) is the main driving force for the binding of the partial agonists to α7-nAChR. The molecular dynamics simulations showed that the opening of the C-loop binding with the partial agonists is in-between the openings for the binding with the full agonist and in the apo state. This conformation difference for the C-loop sheds light on the partial agonism of nAChR.

Keywords Binding energy · Conformation · Homology modeling · MM-GB/SA · Molecular docking

Caijuan Shi and Rilei Yu contributed equally.

C. Shi · S. Shao · Y. Li (✉)
Key Laboratory of Systems Bioengineering,
Ministry of Education, Department of Pharmaceutical Engineering, School of Chemical Engineering and Technology,
Tianjin University,
Tianjin 300072, China
e-mail: liyanni@tju.edu.cn

R. Yu
Division of Chemistry and Structural Biology,
The University of Queensland, Institute for Molecular Bioscience,
Brisbane, Queensland 4067, Australia

Introduction

Nicotinic acetylcholine receptors (nAChRs) are ligand-gated ion channels (LGIC) that mediate fast synaptic transmissions in the central and peripheral nervous systems [1, 2]. These nAChRs are formed by distinctive combinations of five subunits which confer specificity in pharmacological properties and cellular location [3]. The diversity of nAChRs subunits and their assembly is most evident in the central nervous system, in which nine α (α2–α10) and three β (β2–β4) subunits have been identified [4]. Their homomeric or heteromeric assembly generates multiple nAChRs subtypes which differ in their pharmacological and biophysical properties [3].

One of the most important subtypes of nAChRs is α7-nAChR, which is involved in the pathophysiology of several human diseases, such as Alzheimer's disease, Parkinson's disease and schizophrenia [5–7]. Therefore, α7-nAChR has received much interest as a potential target for drug design. However, the high-resolution crystal structure of α7-nAChR is still unavailable. The acetylcholine binding protein (AChBP) which is a structural and functional homologue of the ligand-binding domain (LBD) of α7-nAChR has been used as a model of α7-nAChR [8]. However, AChBP is not a perfect surrogate for α7-nAChR. It lacks the functional transmembrane and intracellular domains to attain all of the conformational states of a functional receptor tethered to an intrinsic membrane channel. Additionally, there is a crucial residue absent in the highly conserved hydrophobic region of AChBP which is present in the same region of α7-nAChR [9, 10]. The structural differences

between AChBP and α7-nAChR result in different binding modes for the ligands that bind with them [8]. In this regard, a direct study of the interactions between α7-nAChR and these ligands is still necessary.

The interactions between full agonists and AChBP have been widely investigated [8]. Previous studies suggest that the agonists are fully enveloped by the protein through hydrogen bonds, cation-π, dipole-cation, and van der Waals interactions with the residues, especially those in the C-loop (β9-β10). In all cases, the ligand-binding specificity is conferred by the non-conserved residues of the complementary subunits [8].

In contrast to full agonists, partial agonists elicit only a fractional pharmacological response, even with full binding site occupation. A ceiling on agonist efficacy can service to reduce the toxicity on overdose and the addiction liability of drugs, if the mechanism and the binding mode are irrespective [9]. In other words, partial agonists possess less toxic, produce fewer side effects and have less addiction liability [11], making them more attractive for the development of drugs. Lape et al. have proposed that the partial agonism in the nAChR superfamily arises from an intermediate pre-opened conformation which has a higher affinity for the agonists than the resting state receptor [12]. Hibbs et al. proposed a schematic representation of the binding modes of the partial agonists, DMXBA (3-(4)-dimethylaminobenzylidine anabaseine), 4-OH-DMXBA (3-(4-hydroxy-2-methoxybenzylidine) anabaseine]) and tropisetron (8-methyl-8-aza-bicyclo[3.2.1]octan-3-ylindoline-3-carboxylate) with AChBP by using conformation analysis of the crystal structure of the AChBP/partial agonist complexes [9]. One of the active metabolites of DMXBA is 4-OH-DMXBA and it possesses higher binding affinity and better partial agonist properties than DMXBA [13]. Tropisetron is a high affinity ligand for α7-nAChR, whereas it is a low affinity ligand for other nAChR subtypes. Tropisetron has been used to alleviate chemotherapy-induced nausea and vomiting [14].

Papke et al. [15, 16] and Macor et al. [17] investigated the efficacy of agonists and partial agonists on α7-nAChR using different experimental methodologies. However, the determinants for the efficacy of these ligands are so complex that there are no explicit reports on them. The purpose of this study is to investigate the interactions of partial agonists and full agonists with α7-nAChR in order to identify the probable determinants for the efficacy of the agonists. To achieve this goal, comprehensive computational simulations on the interactions of the α7-nAChR with two partial agonists, 4-OH-DMXBA and tropisetron and one full agonist, acetylcholine (ACh) were performed based on homology modeling, docking, molecular dynamics simulations and binding energy calculations. The results obtained from this theoretical study will improve our understanding of the efficacy of α7-nAChR agonists and are crucial to the development of more specific therapeutic drugs with fewer side effects.

Methods

Homology modeling

Crysrtal structures of the AChBP in complexes with ACh (PDB ID: 2XZ5) [18], 4-OH-DMXBA (PDB ID: 2WN9) or tropisetron (PDB ID: 2WNC) [9] were used as templates to model the extracellular domain of α7-nAChR. The modeling procedures were similar with those described previously [19].

Molecular docking

The ligands 4-OH-DMXBA, tropisetron and ACh were retrieved from the Protein Data Bank (PDB ID code: 2WN9, 2WNC and 2XZ5, respectively). Prior to minimization, hydrogens were added to these ligands. The non-aromatic ring nitrogen of tropisetron was protonated and charged, whereas it was maintained neutral in 4-OH-DMXBA at physiological pH. All the ligands were minimized by Sybyl 6.92 with Tripos force field and Gasteiger-Huckel charges. The structures of the ligands are shown in Fig. 1. Ligands were docked into α7-nAChR using AutoDock 4.2 [20]. For the ligand dockings, Gasteiger charges were used and the non-polar hydrogens of the macromolecule and the ligands were merged. A grid box with dimensions of $62\times66\times70$ Å^3 and a grid spacing of 0.375 Å was set up by centering on the aromatic box of the binding site. In the docking process, the flexibility of the ligands was considered using a Lamarckian genetic algorithm (LGA) throughout the 25 trials of the GA runs. The complex structures were ranked according to the calculated interaction energy and the quality of the geometric matches. The quality of the geometric matches of the docked binding structures with the lowest binding energies was visually checked and the best one was selected as the initial complex for further studies.

Molecular dynamics simulations

Molecular dynamics (MD) simulations were carried out on the α7-nAChR complexes and on α7-nAChR in the apo state using the Amber 10 [21] package. GAFF and FF03 force field

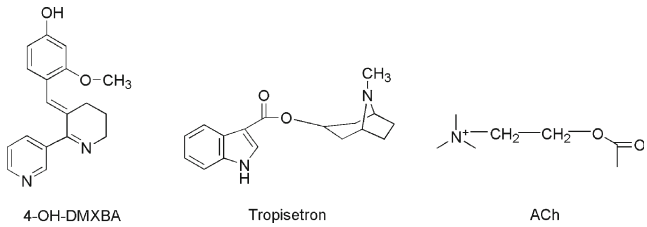

Fig. 1 Chemical structures of the two partial agonists and the agonist

were employed for the ligands and the receptor, respectively. In the molecular dynamics simulations the tropisetron was positively charged, whereas the 4-OH-DMXBA was maintained neutral to be in line with previous experimental study [13, 17]. Prior to the MD simulations, the complex was solvated into an octagon box of TIP3P water molecules and neutralized using Na^+. Then, it was minimized to remove unfavorable van der Waals interactions. The minimization consisted of two steps. First, only the water molecules and ions were minimized with 1000 steps of steepest descent minimization and 1000 steps of conjugate gradient minimization. Second, the restraint on the solute was removed and the whole system was relaxed with 3000 steps of steepest descent minimization and 3000 steps of conjugate gradient minimization. The cutoff of the non-bonded interactions was set to 12 Å for the energy minimization process. After minimization, MD was performed. First, the solute was restrained and the whole system was gradually heated from 10 to 300 K in 20 ps in the NVT ensemble. Then the system was equilibrated in the NPT ensemble where the temperature and pressure were kept at 300 K and 1 atm respectively. Finally, in the production process, the whole system was relaxed and a 10-ns molecular dynamics process was carried out. For all MD steps, the time step was set to 0.002 ps, the particle mesh Ewald (PME) method [22] was applied to deal with long-range electrostatic interactions and the lengths of the bonds involving hydrogen atoms were fixed with the SHAKE algorithm [23].

MM-GB/SA calculation

Binding free energies of each ligand have been computed both with (ΔG_{bind}) and without ($\Delta G'_{bind}$) the inclusion of the entropic term:

$$\Delta G'_{bind} = \Delta E_{VDW} + \Delta E_{ELE} + \Delta G_{SUR}$$

$$\Delta G_{bind} = \Delta E_{VDW} + \Delta E_{ELE} + \Delta G_{SUR} - T\Delta S.$$

For systems without metal ions in the binding sites, calculations using molecular mechanics-generalized Boltzmann surface area (MM-GB/SA) give better results than those using molecular mechanics-Poisson Boltzmann surface area (MM-PB/SA) for ranking the binding affinities of the ligands [24]. So the GB model was used to calculate the binding energy of the ligands. ΔE_{VDW} accounts for the van der Waals term. The eletrostatic interaction (ΔE_{ELE}) is the sum of the desolvation component (ΔG_{GB}) and the Coulombic interaction (ΔE_{EEL}). ΔG_{SUR} is the non-polar desolvation, which is estimated by determining the solvent accessible surface area (SASA). T is the absolute temperature, and ΔS is the entropy of the molecule. $T\Delta S$ contribution can be obtained by performing normal-mode analysis.

Results and discussion

Dynamics of α7-nAChR

The results from the 10 ns molecular dynamics simulations of α7-nAChR, either in the apo state or binding with one of the two partial agonists or with the full agonist, are summarized in Fig. 2. The root mean square deviation (RMSD) values of the backbone atoms relative to the initial structure were calculated to estimate the dynamic stability of these models. Figure 2a shows that the RMSD of the four systems become stable after 2 ns, indicating that they have reached equilibrium. Figure 2b shows the root mean square fluctuation (RMSF) of the Cα for the extracellular domain of α7-nAChR. Interestingly, the overall values of the RMSF of α7-nAChR binding with a partial agonist are larger than those in the apo state or binding with the full agonist, which indicates that the models of binding with the partial agonists fluctuate more significantly than the latter two models in the MD simulations. The larger fluctuation for the partial agonists in the MD suggests the partial agonists probably lack the capacity of the full agonist to stabilize the extracellular domain of the α7-

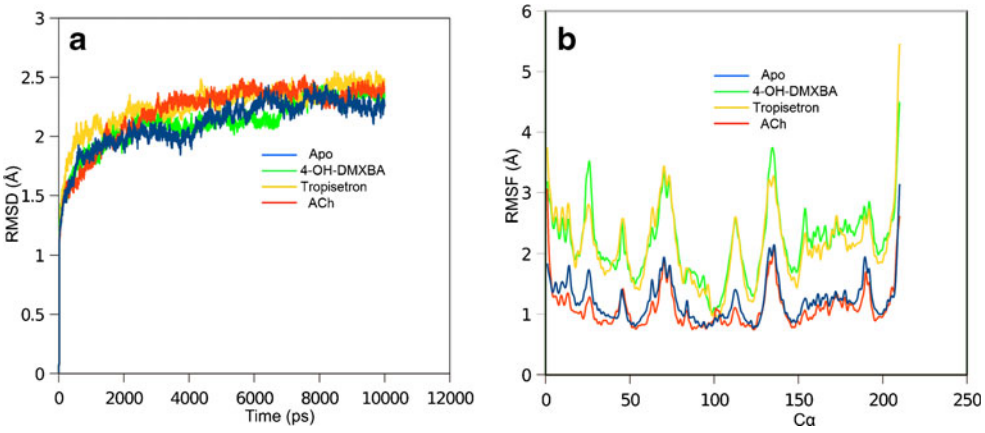

Fig. 2 The RMSD (**a**) and RMSF (**b**) of rat α7-nAChR in the apo state (*deep blue*), in complexes with the partial agonists 4-OH-DMXBA (*green*) or tropisetron (*orange*) or with the agonist ACh (*red*). The values of the RMSD and RMSF are calculated using the Cα of the extracellular domain of α7-nAChR (the average of the five subunits)

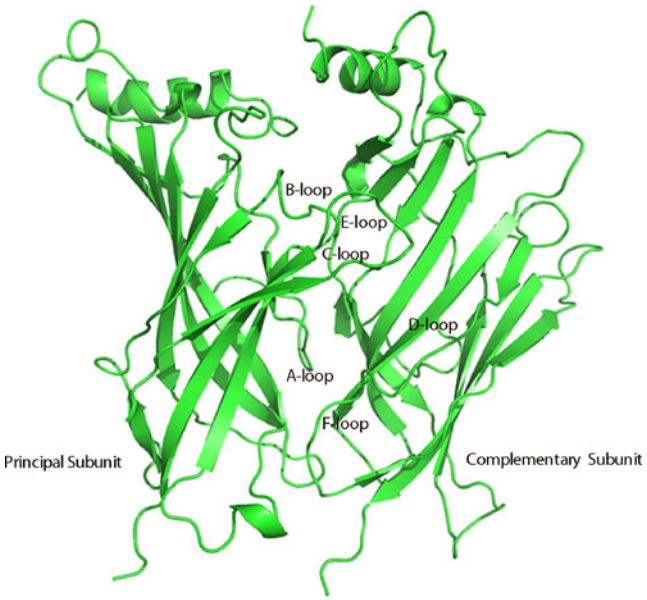

Fig. 3 Overview of the LBD structure of the two subunits of rat α7-nAChR. The structure is shown as a cartoon model. One of the subunits is the complementary subunit, whereas the other is the principal subunit

nAChR into to a stable state, which is necessary for the full activation of the receptor.

Overall views of the structures

α7-nAChR is a homopentamer with five binding sites located at the interfaces between the two subunits of the LBD. Figure 3 shows the secondary structure of one of the five binding sites, which consists of three loops (the A-, B- and C-loops) from the principal subunit and three loops (the D-, E- and F-loops) from the complementary subunit [8].

The geometries of the ligands in the binding sites and the residues of the binding pockets are presented in Fig. 4. As shown in Fig. 4a, ACh is in the center of the aromatic box formed by Trp 55, Tyr 93, Trp 149, Tyr 188 and Tyr 195 of α7-nAChR, with the positively charged nitrogen atom oriented toward the aromatic ring of Tyr 93 to form a cation-π interaction. This result is consistent with an experimental study, in which the aromatic ring of Tyr 93 rather than that of Trp 149 formed a cation-π interaction with ACh [25]. Previously, it was found that in the complex of ACh with AChBP, the acetyl group formed a hydrogen bond with a bridged water molecule [18] but in this model, the acetyl group of ACh is positioned between Gln 57 and Trp 55.

It is not surprising that the binding modes of 4-OH-DMXBA and tropisetron are similar to those in complexes with AChBP in that there is a high sequence identity between α7-nAChR and AChBP in the binding site region (Fig. 4b, c). For 4-OH-DMXBA, Hibbs et al. reported that the side chains of Tyr 93, Trp 147, Tyr 188 and Tyr 195 in the principal subunit and the side chains of Tyr 55 and Ile 118 in the complementary subunit are all involved in the interactions between AChBP and 4-OH-DMXBA [9]. According to the sequence alignment between α7-nAChR and AChBP in the binding site region [26], the corresponding residues in α7-nAChR are Tyr 93, Trp 149, Tyr 188 and Tyr 195 in the principle subunit and Trp 55 and Leu 119 in the complementary subunit, which have been identified as significantly contributing to the affinity of 4-OH-DMXBA with α7-nAChR (Fig. 4b). In the complex of AChBP with tropisetron, the side chains of Tyr 93, Trp 147, Tyr 188 and Tyr 195 in the principal

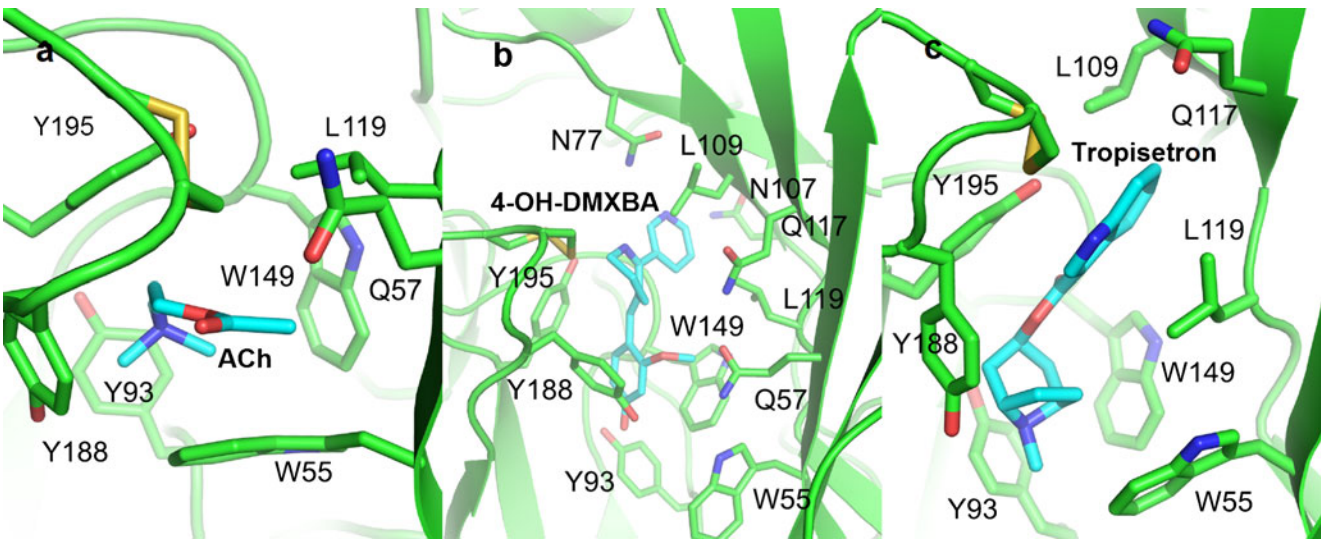

Fig. 4 The binding modes of the ligands in complex with α7-nAChR. **a**, **b** and **c** show the optimum binding modes of ACh, 4-OH-DMXBA and tropisetron in complex with α7-nAChR respectively. The optimum binding mode is defined as the binding mode with the minimum binding energy among the five binding sites of α7-nAChR. The ligands are shown as light blue sticks and the key residues in the binding site are shown as green sticks

subunit and Tyr 55 and Met 116 in the complementary subunit are important to the binding affinity of tropisetron [9]. These residues correspond to Tyr 93, Trp 149, Tyr 188 and Tyr 195 in the principal subunit and Trp 55 and Gln 117 in the complementary subunit [26] in α7-nAChR (Fig. 4c).

Nevertheless, small differences were identified between the binding modes of the 4-OH-DMXBA and tropisetron with α7-nAChR and AChBP. As shown in Fig. 4b, the tetrahydropyridine ring of 4-OH-DMXBA is oriented outside of the binding pocket, whereas it faces toward the binding pocket in AChBP. The slight re-orientation of the tetrahydropyridine ring probably results from a hydrogen bond formed between the nitrogen atom in the pyridine and the side chain of Asn 77, whereas no hydrogen bond is formed between this nitrogen atom and the corresponding residue (Thr 77) in AChBP. In addition, the tetrahydropyridine ring is near Gln 117 in α7-nAChR, which corresponds to the Phe 117 on α4β2-nAChR. Obviously, a hydrophobic side chain residue in this position will form a stronger hydrophobic interaction with 4-OH-DMXBA which explains the higher affinity of 4-OH-DMXBA for binding with α4β2-nAChR (compared with α7-nAChR) [25].

Interestingly, the positively charged nitrogen atom of tropisetron is oriented in a similar position as that of ACh and forms a cation-π interaction with the aromatic ring of Tyr 93. The indole ring of tropisetron is deeper in the binding pocket than it is in the AChBP complex. In the latter, the indole ring is above the Tyr 55 side chain which corresponds to the Trp 55 of α7-nAChR. Compared to Tyr 55, the bulkier side chain of Trp 55 probably occludes the indole ring of tropisetron in the direction of the binding pocket.

MM-GB/SA calculations

The MM-GB/SA method with a single-trajectory was carried out to calculate the binding affinities of the complexes of α7-nAChR with ACh, 4-OH-DMXBA and tropisetron. The binding affinity was averaged for the five subunits. Since the radii of the fluorine and bromine atoms are missing in the MM-GB/SA module of Amber 10, a radii of 1.470 Å for fluorine [27] and 1.850 Å for bromine [28] were added to the GB/SA module.

As shown in Table 1, the binding free energies ΔG_{bind} of ACh, 4-OH-DMXBA and tropisetron are −6.20±1.69, -12.89±2.45 and −17.51±3.61 kcal mol^{-1}, respectively. Hence the theoretical ranking of the binding free energies for the two partial agonists and one full agonist is: ACh<4-OH-DMXBA<tropisetron. According to previous experimental studies, the binding free energies for ACh, 4-OH-DMXBA and tropisetron with rat α7-nAChR are −5.49±0.02, -9.03±0.04 and −11.16±0.30 kcal mol^{-1}, respectively [13, 17, 25, 29], which gives the same ranking as the theoretical prediction.

Table 1 Binding free energy components (kcal mol^{-1}) and standard deviations calculated with MM-GB/SA using structures generated with 10 ns MD simulations in water

Ligand	ΔG_{expt} [a]	ΔE_{VDW}	ΔE_{EEL}	ΔG_{GB}	ΔE_{ELE} [b]	ΔG_{SUR}	$\Delta G'_{bind}$ [c]	TΔS	ΔG_{bind} [d]
ACh	−5.49±0.02	−24.81±0.14	−234.99±0.53	239.86±0.53	4.87±1.06	−3.68±0.01	−23.63±0.16	−17.43±1.53	−6.20±1.69
4-OH-DMXBA	−9.03±0.04	−41.10±0.17	−15.67±0.38	31.02±0.23	15.35±0.46	−5.03±0.01	−29.78±0.21	−16.89±2.24	−12.89±2.45
Tropisetron	−11.16±0.30	−42.03±0.15	−227.36±0.72	237.91±0.75	10.55±1.50	−4.49±0.01	−35.97±0.19	−18.46±3.42	−17.51±3.61

[a] Experimental free energies of binding (kcal mol^{-1}) according to $\Delta G = -RT\ln K_d$

[b] $\Delta E_{ELE} = \Delta E_{EEL} + \Delta G_{GB}$

[c] $\Delta G'_{bind} = \Delta E_{VDW} + \Delta E_{ELE} + \Delta G_{SUR}$

[d] $\Delta G_{bind} = \Delta E_{VDW} + \Delta E_{ELE} + \Delta G_{SUR} - T\Delta S$

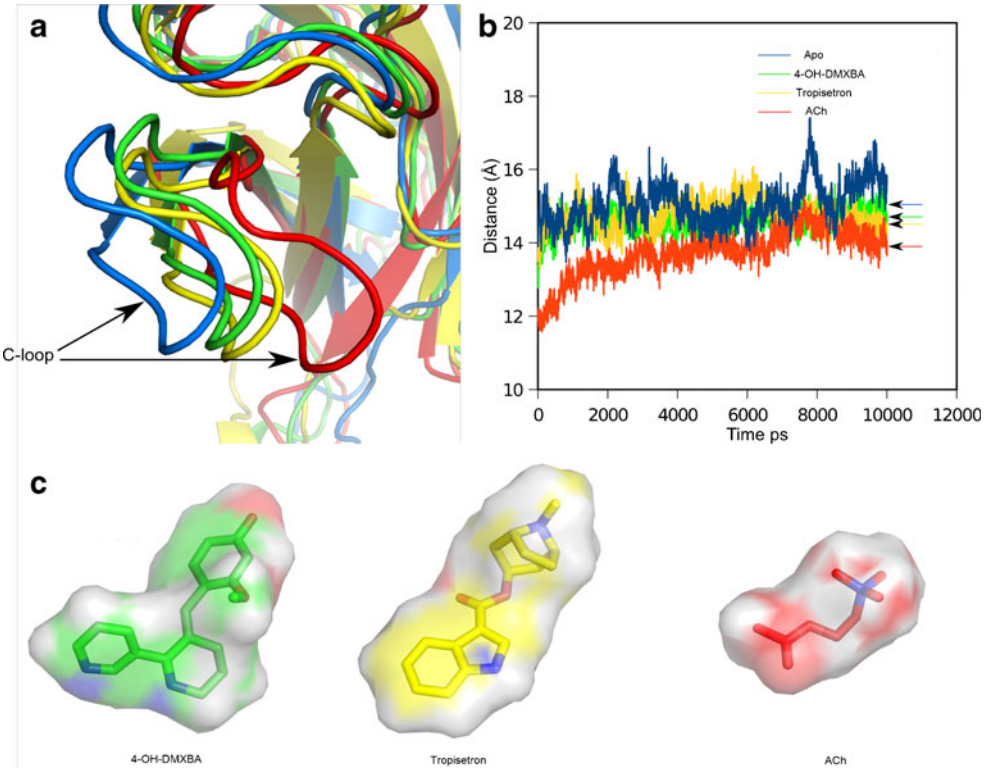

Fig. 5 The opening of the C-loop and the volume of the ligands. **a** the conformation of the C-loop of the α7-nAChR in the apo state (*deep blue*), in complex with the partial agonists 4-OH-DMXBA (*green*) and tropisetron (orange) and in complex with the agonist ACh (*red*). The frames shown in (**b**) were extracted by averaging the final 5 ns of the MD trajectory. **b** the opening of the C-loop is defined as the distance between the two Cα atoms of Cys 190 in the principal subunit and Tyr 32 in the complementary subunit. The arrows indicate the average opening of the C-loop in the 10-ns MD simulations. **c** 4-OH-DMXBA (green), tropisetron (*yellow*), and ACh (*red*) are represented using surface (*transparent*) views to compare the volume

Binding free energy decomposition calculations were performed to evaluate the contribution of van der Waals (vdW), hydrophobic (SUR), electrostatic (ELE) and entropic (TΔS) components to the binding affinities of these ligands. As shown in Table 1, the vdW and SUR terms contribute to the binding affinities of these ligands, whereas the ELE which is comprised of Coulombic electrostatic interactions and polar desolvation energy is unfavorable to the binding of these ligands. Among the two favorable contributions, vdW is stronger than SUR. Therefore, vdW is the main driving force for the binding affinity of the ligands for α7-nAChR. The ELEs of ACh and tropisetron are lower than that of 4-OH-DMXBA which partially accounts for the fact that their potencies are higher than 4-OH-DMXBA. The more preferable electrostatic interaction is probably a result of the cation-π interaction between the positively charged nitrogen atom of ACh and tropisetron. Incorporation of the TΔS term, ΔG_{bind} values become closer to the experimental ΔG_{expt} values when it is compared with $\Delta G'_{bind}$. However, TΔS is by far the contribution with the largest standard deviations compared with other components, highlighting that the inclusion of such a term in ΔG also increases uncertainty.

Table 2 The opening of the C-loops[a], the volumes[b], the molecular weights and the efficacies of the ligands

Ligand	Averaged opening (Å)	Volume ($Å^3$)	Molecular weights	Efficacy (%) (Rat α7-nAChR)
apo	15.06	_	_	0
Tropisetron	14.76	532	298	36
4-OH-DMXBA	14.61	517	291	77
ACh	13.74	293	146	100

[a] The opening is calculated from the 10 ns MD simulations

[b] The volume of the ligands are calculated using web-server (http://3vee.molmovdb.org) built by Voss et al. 2010

Probable determinants on the efficacy of the ligands

A partial agonist possesses a certain ceiling on its efficacy. Typically, the efficacy of ACh is defined as 1 and the efficacies of partial agonists denote the maximal response for a particular agonist/receptor combination under the same conditions [16]. In other words, each partial agonist has a certain maximum efficacy but the factors which influence the efficacy of the partial agonists are complicated. Here we have attempted to determine the probable determinants that affect the efficacy of the agonists.

In comparison with the full agonist ACh, whose efficacy is 1, the efficacies of 4-OH-DMXBA and tropisetron with rat α7-nAChR are 0.47 and 0.36, respectively [16, 17]. A relationship was established between the efficacy of the ligands and the opening of the C-loop and the results are shown in Fig. 5. Interestingly, the extent of the C-loop opening (from large to small) was in the order of the apo state, the complexes with 4-OH-DMXBA, tropisetron and then ACh (Fig. 5a). The same order is shown in Fig. 5b and Table 2 where the opening values are the distances between the two Cα atoms of Cys 190

in the principal subunit and Tyr 32 in the complementary subunit. These results are consistent with previous reports, in which the C-loop of AChBP in the apo state is open, a state corresponding to a closed channel, whereas the C-loop is more closed when it binds with an agonist [26]. Additionally, Hibbs et al. [9] reported that when AChBP bonds with partial agonists, the C-loop is in an intermediate state between open and closed. Overall, the results from this simulation combined with previous experimental studies suggest that the partial agonist fails to fully activate the channel because it lacks the capacity to tightly close the C-loop, which is a hallmark of the activated channels.

The opening of the C-loop in the complexes is probably influenced by the volume of ligands in the binding pocket (Fig. 5c and Table 2). The volumes of two partial agonists are similar to each other, whereas the volume differences between the partial agonist and the full agonist are distinctly different. Indeed, the C-loop becomes more opened with the increasing size of the ligand volume. The high variation similarity between the volume of the ligands and the opening of the C-loop suggests that the ligand volume probably influences the ligand efficacy by influencing the opening of the C-loop. Table 2 lists the molecular weight of the ligands. Obviously, the ligand volume is proportional to the molecular weight. Thus both the molecular weight and the volume of the ligands can be used as an indicator of the efficacy of the ligands.

Besides the volume of the ligands, the efficacy of the ligand is probably also influenced by their binding affinity. A ligand with high efficacy should have preferable binding affinity to the receptor. However, the binding affinity of the ligands cannot be used to evaluate their efficacy. Interestingly, in our system the binding affinity of the ligands has a reverse correlation with their efficacy. As shown in Table 1, the binding affinity of tropisetron is higher than that of 4-OH-DMXBA, and the efficacy of tropisetron on rat α7-nAChR is lower than that of 4-OH-DMXBA (Table 2). These results are not surprising considering that affinity and efficacy are two different parameters. Affinity is a measure of how strongly a ligand binds to a receptor binding site, but in some cases it gives no indication of what effect that binding has on a cell or organism. In fact, a ligand with a high affinity for a receptor does not necessarily have a high efficacy which has been further verified in this study. Therefore, it can be concluded that the efficacy of the nAChR partial agonists is determined by a combination of factors, such as ligand volume, binding affinity and other unknown factors that still need to be determined by further studies.

Conclusions

In summary, four models of α7-nAChR (in the apo state and in complexes with 4-OH-DMXBA, tropisetron and ACh) were built and 10 ns MD simulations were performed on each system. The binding modes that were determined for the two partial agonists and one agonist binding with α7-nAChR are consistent with previous experimental studies. The non-conservative residues in the binding sites influence the different binding modes of these ligands with α7-nAChR and AChBP. Gln 117 was identified to be responsible for the higher binding affinity of 4-OH-DMXBA for α4β2-nAChR over α7-nAChR. Using energy calculation and decomposition, the van der Waals term was discovered to be the major driving force for the three ligands to bind with α7-nAChR. By conformation analysis, the efficacy of the ligands was determined to be related to the volume, the binding affinity and other unknown factors. The results from this study strengthen our understanding of the partial agonism of α7-nAChR and this knowledge can be employed to engineer nAChR partial agonists for neurological therapies.

Acknowledgments The authors acknowledge the support from the Scientific Research Foundation for Returned Overseas Chinese Scholars, State Education Ministry. We are thankful to the Advanced Instrumental Detection & Analytical Center, School of Chemical Engineering and Technology, Tianjin University for providing access to the Sybyl 6.92 software package.

References

1. Changeux JP, Edelstein SJ (2005) Allosteric mechanisms of signal transduction. Science 308:1424–1428
2. Taylor P (2006) Agents acting at the neuromuscular junction and autonomic ganglia. In: Brunton LL, Lazo JS, Parker KL (eds) The pharmacological basis of therapeutics, 11th edn. McGraw-Hill, New York, pp 217–236
3. Novère NL, Corringer PJ, Changeux JP (2002) The diversity of subunit composition in nAChRs: evolutionary origins, physiologic and pharmacologic consequences. J Neurobiol 53:447–456
4. Mao DY, Yasuda RP, Fan H, Wolfe BB, Kellar KJ (2006) Heterogeneity of nicotinic cholinergic receptors in rat superior cervical and nodose ganglia. Mol Pharmacol 70:1693–1699
5. Parri HR, Hernandez CM, Dineley KT (2011) Research update: alpha7 nicotinic acetylcholine receptor mechanisms in Alzheimer's disease. Biochem Pharmacol 82:931–942
6. Burghaus L, Schutz U, Krempel U, Lindstrom J, Schroder H (2003) Loss of nicotinic acetylcholine receptor subunits alpha4 and alpha7 in the cerebral cortex of Parkinson patients. Parkinsonism Relat Disord 9:243–246
7. Levin ED, Rezvani AH (2007) Nicotinic interactions with antipsychotic drugs, models of schizophrenia and impacts on cognitive function. Biochem Pharmacol 74:1182–1191
8. Zouridakis M, Zisimopoulou P, Poulas K, Tzartos SJ (2009) Recent advances in understanding the structure of nicotinic acetylcholine receptors. IUBMB Life 61:407–423
9. Hibbs RE, Sulzenbacher G, Shi J, Talley TT, Conrod S, Kem WR, Taylor P, Marchot P, Bourne Y (2009) Structural determinants for interaction of partial agonists with acetylcholine binding protein and neuronal α7 nicotinic acetylcholine receptor. EMBO J 28:3040–3051
10. Jensen AA, Frølund B, Liljefors T, Krogsgaard-Larsen P (2005) Neuronal nicotinic acetylcholine receptors: structural revelations,

target identifications, and therapeutic inspirations. J Med Chem 48:4705–4745
11. Lagostena L, Trocme-Thibierge C, Morain P, Cherubini E (2008) The partial α7 nicotine acetylcholine receptor agonist S 24795 enhances long-term Potentiation at CA3-CA1 synapses in the adult mouse hippocampus. Neuropharmacol 54:676–685
12. Lape R, Colquhoun D, Sivilotti LG (2008) On the nature of partial agonism in the nicotinic receptor superfamily. Nature 454:722–727
13. Kem WR, Mahnir VM, Prokai L, Papke RL, Cao X, LeFrancois S, Wildeboer K, Prokai-Tatrai K, Porter-Papke J, Soti F (2004) Hydroxy metabolites of the Alzheimer's drug candidate 3-[(2,4-dimethoxy)-benzylidene]-anabaseine dihydrochloride (GTS-21): their molecular properties, interactions with brain nicotinic receptors, and brain penetration. Mol Pharmacol 65:56–67
14. Ho KY, Gan TJ (2006) Pharmacology, pharmacogenetics, and clinical efficacy of 5-hydroxytryptamine type 3 receptor antagonists for postoperative nausea and vomiting. Curr Opin Anaesthesiol 19:606–611
15. Papke RL, Papke JPK (2002) Comparative pharmacology of rat and humana7 nAChR conducted with net charge analysis. Br J Pharmacol 37:49–61
16. Papke RL, Schiff HC, Brian AJ, Horenstein NA (2005) Molecular dissection of tropisetron, an α7 nicotinic acetylcholine receptor-selective partial agonist. Neurosci Lett 378:140–144
17. Macor JE, Gurley D, Lanthorn T, Loch J, Mack RA, Mullen G, Tran O, Wright N, Gordon JC (2001) The 5-HT_3 antagonist tropisetron (ICS 205–930) is a potent and selective α7 nicotinic receptor partial agonist. Bioorg Med Chem Lett 11:319–321
18. Brams M, Gay EA, Saez JC, Guskov A, van Elk R, van der Schors RC, Peigneur S, Tytgat J, Strelkov SV, Smit AB, Yakel JL, Ulens C (2011) Crystal structures of a cysteine-modified mutant in loop D of acetylcholine-binding protein. J Biol Chem 286:4420–4428
19. Yu RL, Craik DJ, Kaas Q (2011) Blockade of neuronal alpha7-nAChR by alpha-conotoxin ImI explained by computational scanning and energy calculations. PLoS Comput Biol 7,e100201
20. Morris GM, Goodsell DS, Halliday RS, Huey R, Hart WE, Belew RK, Olson AJ (1998) Automated docking using a Lamarckian genetic algorithm and an empirical binding free energy function. J Comp Chem 19:1639–1662
21. Case DA, Darden TA, Cheatham TE III, Simmerling CL, Wang J, Duke RE, Luo R, Merz KM, Pearlman DA, Crowley M, Walker RC, Zhang W, Wang B, Hayik S, Roitberg A, Seabra G, Wong KF, Paesani F, Wu X, Brozell S, Tsui V, Gohlke H, Yang L, Tan C, Mongan J, Hornak V, Cui G, Beroza P, Mathews DH, Schafmeister C, Ross WS, Kollman PA (2008) AMBER 10. University California, San Francisco
22. Darden T, York D, Pedersen L (1993) Particle Mesh Ewald - an N.Log(N) method for ewald sums in large systems. J Chem Phys 98:10089–10092
23. Giccotti G, Berendsen HJC, Ryckaert JP (1977) Numerical-integration of Cartesian equations of motion of a system with constraints -molecular-dynamics of N-Alkanes. J Comput Phys 23:327–341
24. Hou TJ, Wang JM, Li YY, Wang W (2011) Assessing the performance of the MM/PBSA and MM/GBSA methods. 1. The accuracy of binding free energy calculations based on molecular dynamics simulations. J Chem Inf Model 51:69–82
25. Puskar NL, Xiu X, Lester HA, Dougherty DA (2011) Two neuronal nicotinic acetylcholine receptors, α4β4 and α 7, show differential agonist binding modes. J Biol Chem 286:14618–14627
26. Hansen SB, Sulzenbacher G, Huxford T, Marchot P, Taylor P, Bourne Y (2005) Structures of aplysia AChBP complexes with nicotinic agonists and antagonists reveal distinctive binding interfaces and conformations. EMBO J 24:3635–3646
27. Bondi A (1964) van der Waals Volumes and Radii. J Phys Chem 68:441–451
28. Riley KE, Merz KM (2007) Insights into the strength and origin of halogen bonding: the halobenzene-formaldehyde dimmer. J Phys Chem A 111:1688–1694
29. Talley TT, Yalda S, Ho KY, Tor Y, Soti FS, Kem WR, Taylor P (2006) Spectroscopic analysis of benzylidene anabaseine complexes with acetylcholine binding proteins as models for ligand nicotinic receptor nteractions. Biochem 45:8894–8902